Development of Geiger Mode Micro-Avalanche Photodiode Arrays for FiberGLAST

Stefan Vasile[*a], Denis Shamo[a] , Suzanne Shera[a], Gerald J. Fishman[b]
[a]Radiation Monitoring Devices, Inc., 44 Hunt Street, Watertown, MA 02466
[b]Marshall Space Flight Center, Huntsville, AL 35812

ABSTRACT

The Gamma-Ray Large Area Space Telescope (GLAST) mission is planned as the next major challenge in high-energy astrophysics. FiberGLAST is one of the technologies being developed for GLAST and is using arrays of scintillation fibers (>100,000) for the pair-tracking and calorimeter detectors. The instrument requires optical detectors with high gain, low cost, and low power to read out the large number of individual fibers.

We evaluated the feasibility of using Geiger mode operated micro-Avalanche Photodiode (μAPD) arrays in conjunction with optical concentrator arrays as scintillating fiber readouts for FiberGLAST. The μAPD detection efficiency and dark count rate were measured for different μAPD configurations and temperatures. Prototype concentrators were fabricated and the light losses evaluated. Additionally, low power, simple passive quenching circuits for μAPDs were investigated. Using the components' measured performance, we analyzed the tradeoffs between the concentrator light transfer efficiency, μAPD sensitive area, and speed, in order to maintain high detection efficiency at preset dark count rates.

We found that there is a minimum size of the μAPD sensitive area required to operate the integrated μAPD-concentrator detector at high detection efficiency (>90%). Cone concentrators, of potentially low cost, would allow for the fabrication of μAPDs with smaller areas, and consequently reduced dark count rate. Active load passive quenching has both decreased the μAPD reset time from 10 to 1 μs and has resulted in 0.7 μW /pixel quiescent power. We concluded that fibers ranging from 0.3 to 0.7 mm can be efficiently read out by the integrated detector, while maintaining less than 100 Hz dark count rate. The predicted μAPD concentrator performance meets most of the requirements and makes these detectors promising candidates for the readout of the scintillating fibers at FiberGLAST.

Keywords: FiberGLAST, Geiger, avalanche photodiode, concentrator.

1. INTRODUCTION

Advanced detectors, detector arrays, and readout electronics are needed to support the next generation of Earth, space, planetary, and life science missions. Space-borne detector systems are being designed to study gamma-ray bursts, which are among the most intense emissions in the sky.[1] The detection of this high-energy cosmic radiation will provide information about stars in the most distant reaches of our galaxy or an entirely new class of objects near the edge of the observable Universe. New gamma ray telescope designs, based on scintillating fiber arrays, could provide low cost, high resolution, lightweight, very large area, radiation-hard and multi-radiation length instrumentation for mapping the gamma-ray bursts. FiberGLAST is one of the technologies being developed for GLAST and is using orthogonal arrays of numerous scintillation fibers. To exploit the spatial resolution performance intrinsic to scintillating fiber detectors, optical detectors with single photon sensitivity and fast response are required to readout the faint light signal produced by the individual fibers. Furthermore, the large number of detectors required may dramatically increase the power requirements, the complexity of the electronics, and, hence, the cost. The silicon avalanche photodiode (APD), with internal gain and rugged construction, is one of the candidates that may fulfill the requirements of high-efficiency, high gain, low cost, and low power optical detectors.

RMD is a commercial manufacturer of high-quality APDs. Two state-of-the-art technologies at RMD produce high-gain, silicon-based APD arrays. The first technology produces APD structures with deep diffusions (typically in the 20 to 50 μm range) resulting in gains as high as 40,000 and excellent noise performance (6 e-h pairs) when operated in the proportional mode at approximately -70°C.[2] The second technology (the μAPD technology) utilizes the planar process to fabricate Geiger mode operated, small pixel size (10 – 180 μm) devices. In the Geiger mode, the breakdown is initiated by single carriers

[*] Correspondence: Email: svasile@rmdinc.com; WWW: http://www.rmdinc.com; Telephone: 617 926 1167; Fax: 617 926 9980

crossing the high electric field of the **p-n** junction. When operated in Geiger mode, these μAPDs exhibit gains as high as 10^9 at room temperature, an output signal in the volt range, and are capable of detecting single photons.[3,4] The devices are rugged and tolerate high illumination levels without apparent loss of performance. Passive quenching, the simplest way to interrupt the Geiger avalanche, results in 10-30 μs reset time. The sensitivity of silicon μAPDs matches well the spectral output of the scintillating fibers; therefore, their single photon detection capability at these wavelengths and low quiescent operation power makes them an ideal candidate for the FiberGLAST application.

The goal of this work was to examine the feasibility of developing a novel optical detector for FiberGLAST, based on the current μAPD technology and concentrators. Our objectives were to estimate the μAPD's significant characteristics, identify tradeoffs, and investigate alternative array configurations according to the following specifications: (1) scintillating fibers with diameters ranging from 250 -700 μm; (2) optical signals at the end of the scintillating fibers of 10-20 photons per scintillation event; (3) spectral output ranging from 450-650 nm thus matching the peak emission for the most common scintillating fibers; (4) optical signal pulse widths (at the APD input) of 20 nsec; (5) APD reset time < 1μsec; and (6) an optical signal event rate < 100 Hz; and (7) moderate cooling (minimum temperature -30 °C).

2. KEY ELEMENTS OF THE TECHNOLOGY

Avalanche photodiodes, operated in proportional mode, can be considered for fiber detector readouts. However, their relatively large size and generation volume (compared to our μAPD array concept) leads to a high dark count rate when operated in the Geiger mode at room temperature, or requires low noise amplification and cooling when operated in proportional mode. Our μAPD technology minimizes the size of the sensitive area and generation volume and results in low dark count rates when operated in Geiger mode. In order to maintain the μAPD's low dark count rate advantage, the arrays have to be interfaced to the larger size scintillating fibers by using concentrator optics.

The use of microlens array technology, in conjunction with our μAPD array, works well for small divergent rays, but fails to efficiently concentrate the rays emitted at large divergent angles. Concentrators, as opposed to microlenses, are non-imaging optical devices, which efficiently confine light for large input numerical aperture (NA) of today's commercially available scintillating fibers.[5]

The novel scintillating fiber detector will use μAPDs in conjunction with integrated optical concentrators, which are optically coupled to the scintillating fibers. The concentrator array will be aligned and cemented to the sensitive area of the APD pixels. This concept promises to preserve the advantages of the μAPD design while increasing the optical signal available for detection. Integration of the concentrator arrays with μAPD arrays will result in an optical detector with reduced noise, photon detection capability, low quiescent power, output in the volt range and will alleviate the need to use pixel level, low-noise preamplifiers. Figure 1 shows the engineering solution to the proposed concept.

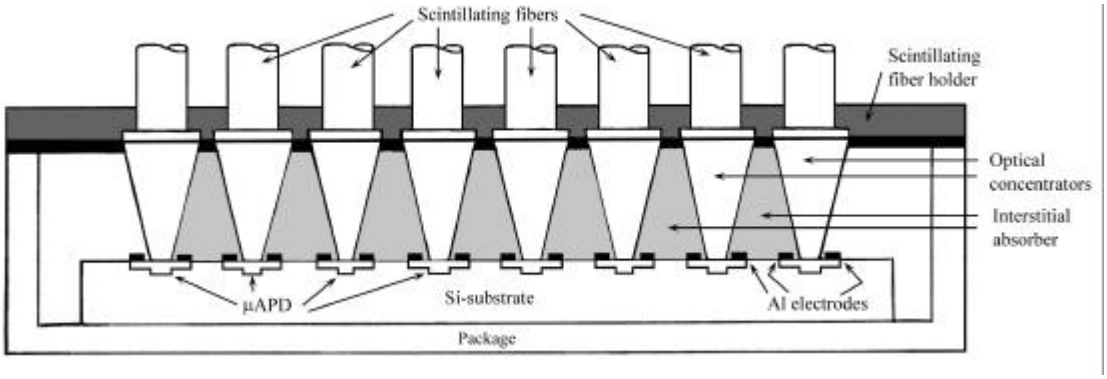

Figure 1**.** View of the envisaged integrated detector array. A coherent array of concentrators will be aligned and cemented to the sensitive area of the μAPD pixels. Scintillating fibers are aligned to the concentrator arrays using a fiber connector. Quenching circuits may be mounted in the same package with the μAPD array, thus resulting in a compact, multi-chip module.

Our analytical approach is to evaluate the tradeoffs between the concentrator's light transfer efficiency and the μAPD area, while preserving a high detection efficiency and low quiescent power of the composite *mAPD – concentrator* detector. In this section, we will present the key elements of the proposed detector technology and the performance of the detector components.

2.1. The μAPD

The **p-n** semiconductor junction μAPD is designed to minimize the number of thermally generated carriers by decreasing the generation volume of the space charge region. The design results in dark count rates as low as 100 Hz on 20 μAPDs at room temperature and low operation voltage (30 - 40 V). The measured single photon detection efficiency in the green-red wavelength range (typical for today's scintillating fibers) is 20% at room temperature. The passive quenching scheme (a high value resistor in series with the photodiode) provides 1-3 V signal amplitude output pulses with approximately 10 μs width, and can drive standard 5 V logic circuitry without further amplification. If faster timing is needed, active quenching designs can be implemented.[6] We have developed active quenching circuits, which drive μAPDs operated in the Geiger mode with 5 ns rise and fall time, thus improving by more than two orders of magnitude the APD speed and, hence, the maximum detection rate.[2] However, for a 5ns reset time, the quiescent power / Geiger pulse increases to the mW range and further circuitry improvements do not promise a dramatic power reduction. Because FiberGLAST requires numerous fibers and the power is limited to approximately 300 W, tradeoffs between speed, cost and power will have to be worked out.

2.2. The Cone Concentrator

The concentrator we plan to use for the FiberGLAST application is the cone concentrator, shown in Figure 2a. Light is channeled to the fiber tip through multiple reflections. The input aperture of the concentrator is $NA_{in}=NA_{out} \times D_{out}/D_{in}$, where NA_{out} is the output aperture, D_{out} is the exit aperture diameter, and D_{in} the concentrator input diameter. The propagation ray to the fiber exit surface can be re-constructed if we repeatedly image the axial section of the fiber in the tangential plane, as represented by the broken lines. Ray 1 crosses the image surface and consequently hits the detector, while ray 2 is back-reflected. The concentrator's performance is characterized by the concentration factor CF (CF = (*input area)/(output area)*) and the light transfer efficiency. Using the ray tracing depicted in Figure 2a, we evaluated the maximum CF for concentrators matching NA of single-clad and multiclad Bicron scintillating fibers, [7] and the results are shown in Table I (point sources were assumed for the maximum CF calculation).

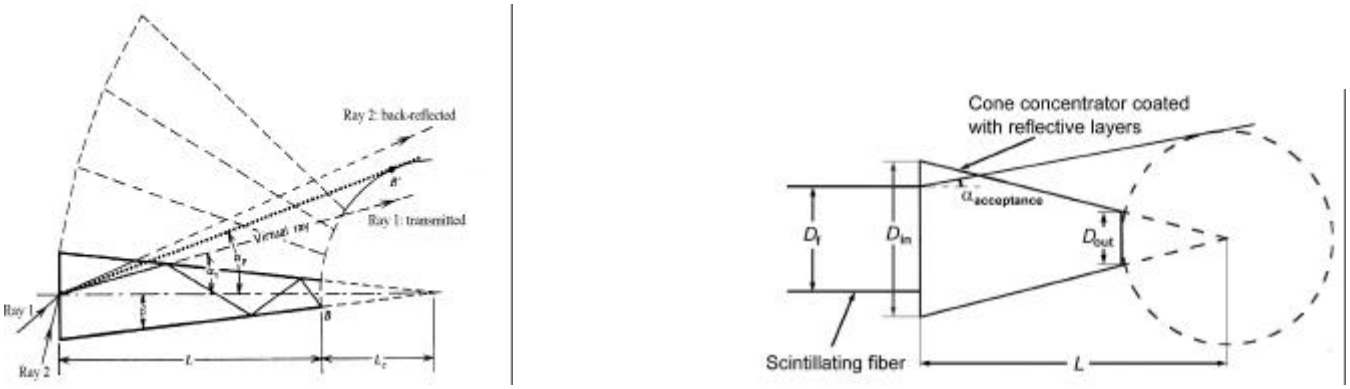

(a) (b)

Figure 2(a). Schematic of the ray tracing through a cone concentrator for point light sources.[8] The dashed circle represents a hypothetical line, defining the boundary outside of which the incident rays will be back-reflected to the concentrator input; (b) Schematic of the cone concentrator with a scintillating fiber coupled to the entrance aperture. The line tangent to the dashed circle defines the maximum acceptance angle, $\alpha_{acceptance}$, of the cone concentrator. Rays within the acceptance angle will be propagated through the concentrator to the exit aperture and will result in full collection of the generated light at the input aperture (assuming no reflection losses).

Table I.

Clad	n_{core}	n_{clad}	NA	$\alpha_{acceptance}$	D_{out}/D_{in}	Concentration Factor
Single	1.6	1.49	0.58	21	0.362	7.8
Multi	1.6	1.42	0.74	27	0.462	4.8

In order to evaluate the degree to which the concentrator's NA will match the scintillating fiber's numerical aperture, we calculated the dependence of the maximum acceptance angle on the concentration factor for cone concentrators coupled to scintillating fibers of diameter D_f (shown in Figure 2 b) and plotted the results in Figure 3 for 20 mm long cone concentrators. The results show that the concentration factors are somewhat lower when compared to the point source case and their dependence on the scintillationg fiber diameter is weak.

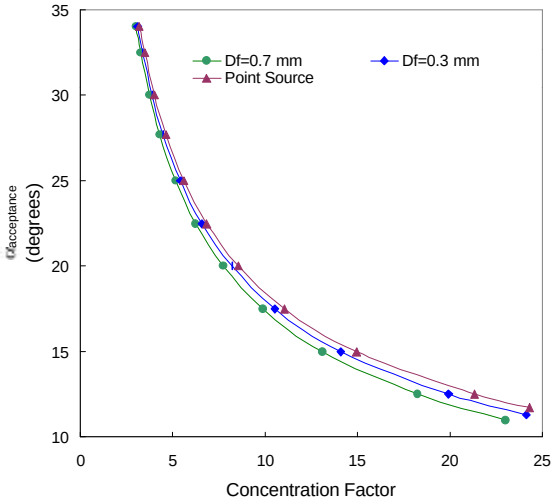

Figure 3. Calculated maximum acceptance angle versus the concentration factor for different fiber diameters. For high concentration factors, the acceptance angle will be smaller than the incident angle of the rays emitted by the scintillating fiber, and consequently light losses will occur due to back-reflection.

3. EVALUATION OF THE COMPONENTS' PERFORMANCE FOR FIBERGLAST

In order to assess the *mAPD-concentrator* performance, we evaluated separately the μAPD and cone concentrator performance based on existing μAPD devices and fabricated concentrator prototypes. We measured the μAPD characteristics (dark count rate, reset time and detection efficiency) and extrapolated the data to the expected operation range. Prototype concentrators were fabricated and the concentration efficiency was measured for different output aperture diameters. Also, we investigated simple, low-cost quenching circuits meeting the reset time requirements. Based on the measured performance of the μAPDs and concentrators, we generated parametric curves and analyzed the operating characteristics of the composite sensor in order to determine the operation conditions meeting the FiberGLAST performance requirements.

3.1. μAPD Detection Efficiency vs. Number of Photons

The detection efficiency was measured using pulsed LEDs emitting at 570 nm wavelength, matching the spectral emission of green fibers. The detection efficiency dependence on photon density is shown in Figure 4 for different voltages, applied above the breakdown voltage (the breakdown voltage is approximately 40V). The detection efficiency increases monotonically with the number of photons/pulse and reaches approximately 98% at 12 photons/pulse. The data were fitted to the detection efficiency equation $DE = 1 - \exp(-P_b * QE * n_f)$, where DE is the detection efficiency, P_b is the breakdown probability, QE is the μAPD quantum efficiency, and n_f is the average number of photons / pulse. This analytical expression will be used to evaluate the tradeoffs between sensitivity, speed, and quiescent power.

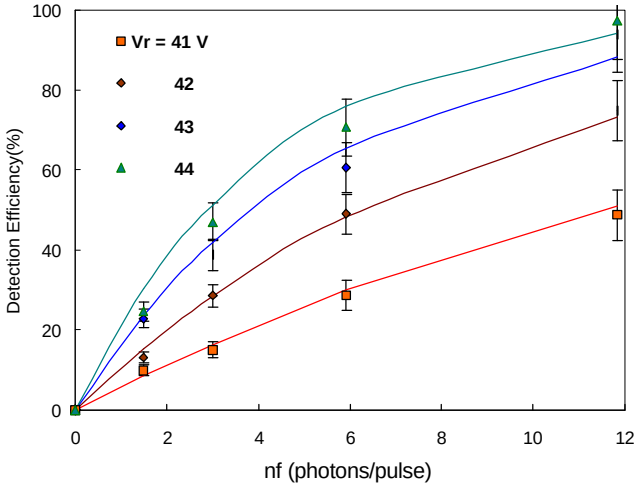

Figure 4. Room temperature measured μAPD detection efficiency versus the number of photons, n_f, incident on the sensitive area. The experimental data are fitted with a saturation-type function.

3.2. **Active Load Quenching**

The reset time, defined as the total Geiger pulse width at 10% of the peak value (i.e. *rise time + fall time*), was measured for standard passive quenching mode and active load quenching. The active load quenching circuit is a high frequency bipolar transistor biased in a common emitter configuration with a resistor in the emitter circuit. The voltage developed across this resistor during the avalanche raises the base potential and decreases the μAPD bias below the breakdown voltage, thus quenching the avalanche. The measured reset time and the energy/Geiger pulse versus the emitter resistance are shown in Table II**.** All the measurements were performed at 3.5 V above the breakdown voltage, except for the 0.5 kΩ load (due to the low voltage drop on the resistive load, the allowed over-voltage was less than 3 V). The recorded Geiger pulse shapes for 20 and 1 kΩ resistors are shown in Figures 5(a) and 5(b). For 1 kΩ resistors, the active load quenching improves the reset time to 0.9 μs and requires only 0.7 μW at 100 Hz dark count rate. The reset time meets the FiberGLAST timing requirements, while the low quiescent power requires only a fraction of the power allotted for the FiberGLAST for 100,000 scintillating fibers.

In anticipation of the expected APD size for the FiberGLAST application (150 – 300 μm), we measured the dependence of the reset time for active load quenching for the existing 10, 20, 30 and 180 μm diameter μAPDs. The results showed a weak dependence of the reset time on the μAPD diameter (the reset time increases by approximately 15% over the whole diameter range). Based on the above results, we believe that an optimized μAPD - high frequency transistor pair could preserve the reported temporal performance of the active load quenching. Higher current gains will early quench the Geiger avalanche and avoid Geiger charge build-up in the μAPD (high charge density is primarily responsible for capacitance modulation and long fall times). Our plans are to refine the μAPD SPICE model parameters and, thus, to predict the μAPD - active load quenching circuit transitory behavior over an extended μAPD diameter range.

Table II. Measured reset time and energy/pulse on 30 μm diameter μAPDs for passive and active load quenching.

Mode	Emitter Resistance	Reset Time	Peak Current	Energy/ pulse	Quiescent Power @ 100Hz
	kΩ	μsec	μA	nJ	μW
Passive quenching	100	20	0.03	1.5	0.2
Active Load Quenching	20	14	0.2	5.1	0.5
Active Load Quenching	6	4.0	0.5	4.8	0.5
Active Load Quenching	3	2.1	1.1	4.7	0.5
Active Load Quenching	1	0.9	3.4	7.0	0.7
Active Load Quenching	0.5	0.5	6.1	7.0	0.7

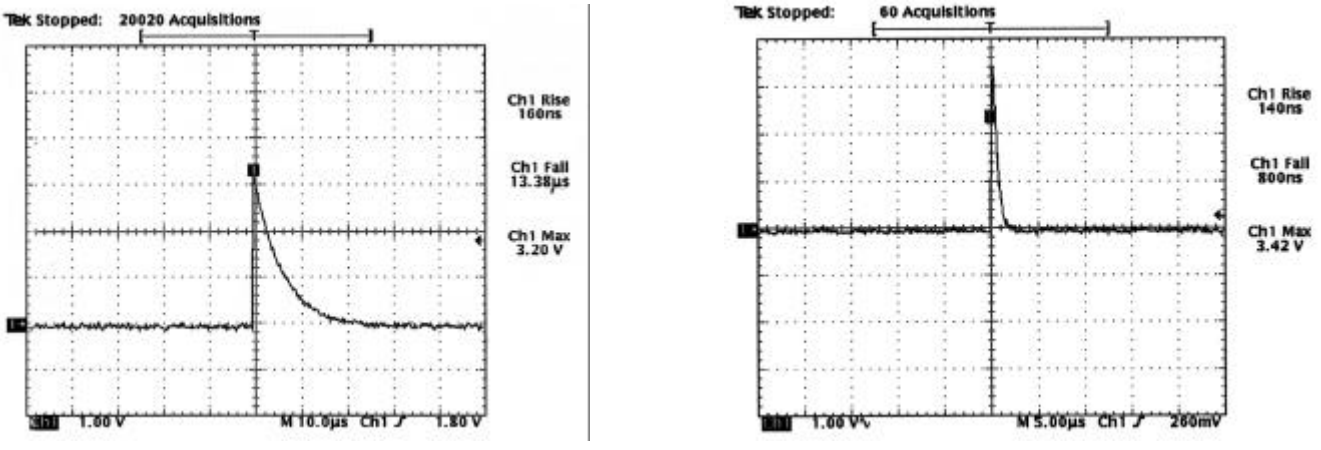

(a) (b)

Figure 5 (a). Geiger pulse passively quenched using an active load quenching circuit with 20 kΩ resistors for 30 μm diameter μAPDs. The reset time is 14 μs (horizontal scale is 10μsec/div); (b) Active load quenched pulse with 1 kΩ active load (horizontal scale is 5 μsec/div). The reset time is 940 ns, and meets the FiberGLAST timing specification.

3.3. µAPD Pixel to Pixel Crosstalk

It is widely accepted that the origin of crosstalk in the Geiger-mode-operated APDs is light emission in the semiconductor due to "hot" carrier generation during the avalanche multiplication process.[9] Carrier thermalization generates optical photons that travel in the semiconducting material to the neighboring APD pixels (*internal* crosstalk) and initiate false Geiger events. The *external* crosstalk occurs through the emission of light out of the semiconductor material and back reflected onto the adjacent pixels. Fortunately, the use of concentrators with interstitial absorbers (see Figure 1) will prevent external light scattering to the neighboring pixels and will not induce sizeable external crosstalk. To determine the internal crosstalk in the µAPD arrays, Geiger pulses were generated in one pixel (*source* pixel) at a known rate and the count rate modification in the neighboring pixels (*receiver*) was monitored. Crosstalk was defined as the correlated counting rate change in the *receiver* pixel normalized to the Geiger rate in the *source* pixel:

$$\text{Crosstalk} = \frac{\text{DarkRate}(\text{sourceON}, \text{receiverON}) - \text{DarkRate}(\text{sourceOFF}, \text{receiverON})}{\text{DarkRate}(\text{sourceON}, \text{receiverOFF})} \qquad (1)$$

(here OFF/ON mean bias below/above the breakdown voltage).

We measured the dark count rate for the above bias situations, up to a voltage corresponding to the detection efficiency saturation condition, and for different pixel *center-to-center* spacing. The evaluated crosstalk for different bias conditions *versus* the distance between pixels is shown in Figure 6. As the FiberGLAST design will use fibers with diameter greater than 500 µm,[10] the measured crosstalk will not significantly contribute to the background dark count rate.

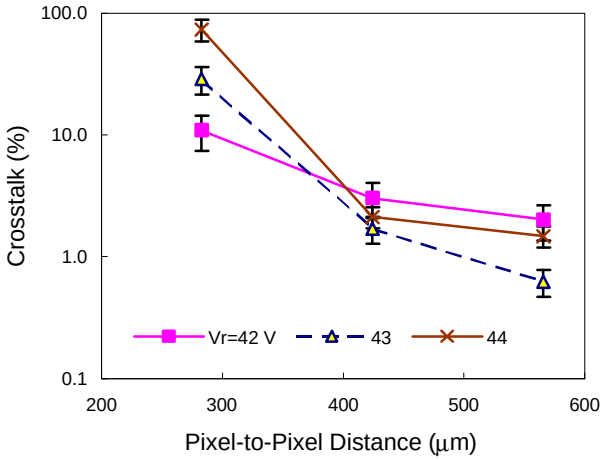

Figure 6. The dependence of the crosstalk on the distance between µAPD pixels. The crosstalk was measured up to a voltage corresponding to the detection efficiency quasi-saturation condition. The crosstalk is less than 10% for pixel pitch greater than 380 µm and decreases to approximately 2% for pitch sizes larger than 450 µm.

3.4. Extrapolation of the measured dark count rate data

One important question we have to answer is how to accurately predict the µAPD optimal sensitive area, and the operating temperature resulting in less than 100 Hz dark count rate, using measurements on existing µAPDs. In order to predict the performance in the optimal *temperature- mAPD size* range, we measured: (1) the dark count rate at room temperature for three different µAPD sizes and applied geometrical corrections to determine the effective APD avalanche area (the dark count rate is proportional to the effective avalanche area), and (2) the dark count rate over a wide temperature range, and evaluated the activation energy for different applied bias voltages.

3.4.1. Geometrical Corrections to the µAPD Avalanche Area

Due to the planar diffusions used in the µAPD fabrication, the electric field intensity at the avalanche area edge is lowered and results in an effective shrinkage of the avalanche region. In order to evaluate the effective avalanche area, we calculated the electric field profile across the avalanche junction, and the avalanche ionization probability profile for electrons (electrons

are known to dominate the avalanche phenomenon due to their higher ionization probability). The effective avalanche region diameter is empirically defined at the half-width of the ionization integral spatial profile and is 27 μm for a 30 micron geometrical diameter μAPD. This result will be factored in the dark rate calculations and will help to accurately predict the dark count rate for larger μAPD diameters.

3.4.2. μAPD Dark Rate Extrapolation to Low Temperatures

We measured the dark count rate at different temperatures down to – 29 °C on 30 μm diameter μAPDs biased at different voltages, and evaluated the activation energy of the Geiger avalanche. As shown in Figure 7**,** based on the calculated activation energy, we extrapolated the dark count rate to lower temperatures (Figure 7)**.** This result will provide the basis for the evaluation of the required operating temperature for a particular μAPD area.

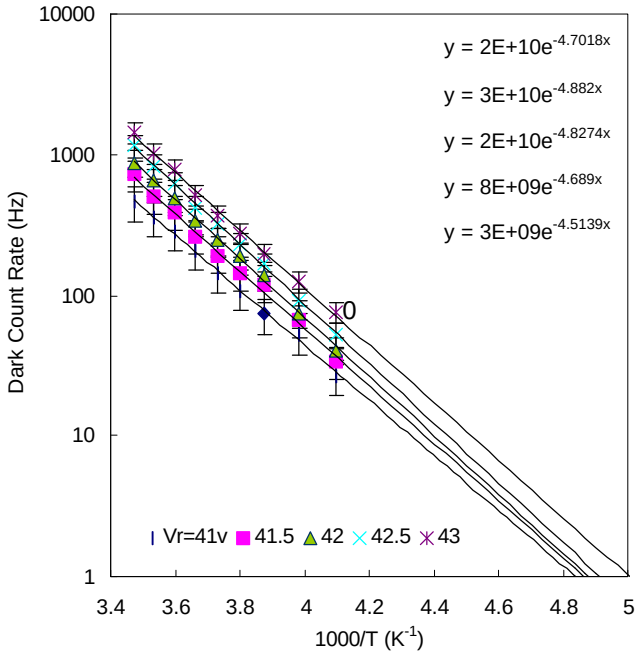

Figure 7. Measured and extrapolated dependence of the dark count rate on temperature for 30 μm diameter μAPD. Inserts show the fitted analytical functions associated with each applied voltage. These analytical functions will be used to predict the overall μAPD-concentrator performance. The top inserted function corresponds to the highest applied voltage (43 V).

3.5. Cone Concentrator Performance

To test the performance of cone concentrators, we fabricated a few cone concentrator prototypes with 1mm diameter input aperture and various exit aperture diameters, and measured the light concentration efficiency for different concentration ratios. The cone concentrators were pulled using 1mm diameter, optical quality silica fibers heated at approximately 650°C. The conic surface was coated with Al or an In:Ga alloy to create the mirror surface. Cone concentrators were spliced to 1 mm Bicron, BCF 20, multiclad scintillating fibers emitting green photons (see Figure 8a). The scintillating fiber was excited with an UV lamp and the concentrated light at the silica fiber tip end was measured on a silicon photodiode with 1.2 mm diameter of the active area, coupled to the concentrator tip using an index-matching optical fluid. The light transfer efficiency is shown in Figure 8b, was fitted with an exponential decay function (Figure 8b insert) for two concentrators and resulted in an averaged exponential factor of -0.1045. This function will be used to evaluate the photons available for detection on the μAPD, and will be factored into the overall detection efficiency calculations. No measurements are available at this time on In:Ga coated concentrators. We expect lower reflectance on these concentrators as the In:Ga alloy has lower reflectivity (approximately 80%) as compared to the Al films (>95%). However, we will consider this alloy further as a candidate for the mirror surface preparation, because the mirror surface quality is less sensitive to the cone surface defects, and the mirror deposition cost is very low.

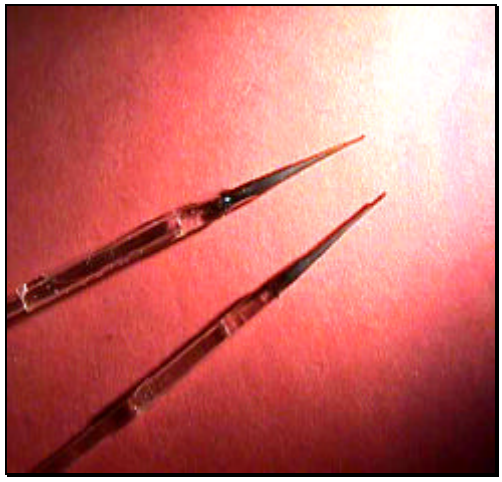

(a)

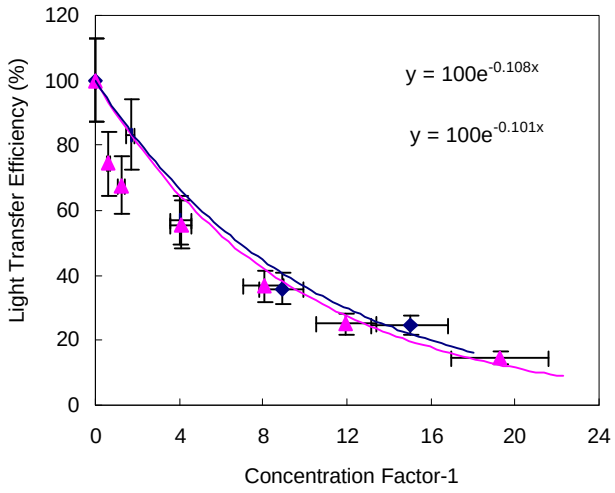

(b)

Figure 8(a). Photograph of the prototype fiber cone spliced to 1mm scintillating fibers. The diameter of the cone concentrator tip is 0.25 mm; (b) Measured light transfer efficiency versus the concentration factor CF for two prototype cone concentrators (symbols) and interpolated exponential functions (solid lines) show low spreading of the concentrating efficiency values for CF>4. The inserted equations show the exponential factors for both curves. The efficiency is lower when compared to the calculated values, as we would expect 100% light transfer efficiency at concentration factors of 4. This 40% loss is mainly due to inherent reflection losses and the quality of the aluminum mirror coating at the cone concentrator surface (see Table I for multiclad fibers).

4. THE OPERATING CHARACTERISTICS OF μAPD-CONCENTRATOR ARRAYS

Based on the above measured performance of the μAPD arrays and cone concentrators, we generated the analytical functions necessary to evaluate the overall performance of the integrated *APD-concentrator* array over an extended temperature and μAPD diameter range, and developed a program to determine the μAPD optimal size. The program uses as inputs the measured performance of existing concentrators and μAPD devices, the fiber's emission yield and numerical aperture, and outputs the expected dark count rate and detection efficiency. Single-clad and multiclad scintillating fibers with 8,000 photons/MeV scintillation yield, 1 m long, and 3.5 m attenuation length, were assumed as light sources for the *concentrator-mAPD* detector performance predictions.[7] The results are summarized in Figures 9-10**.**

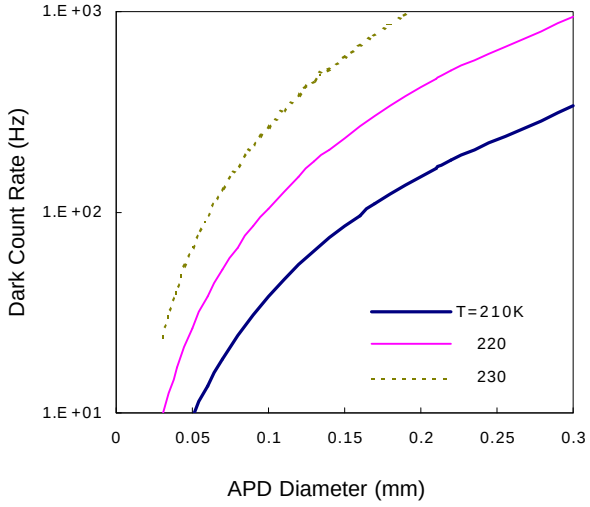

Figure 9. Predicted μAPD dark count rate versus the μAPD diameter at 3 V applied bias above the breakdown voltage for three operating temperatures.

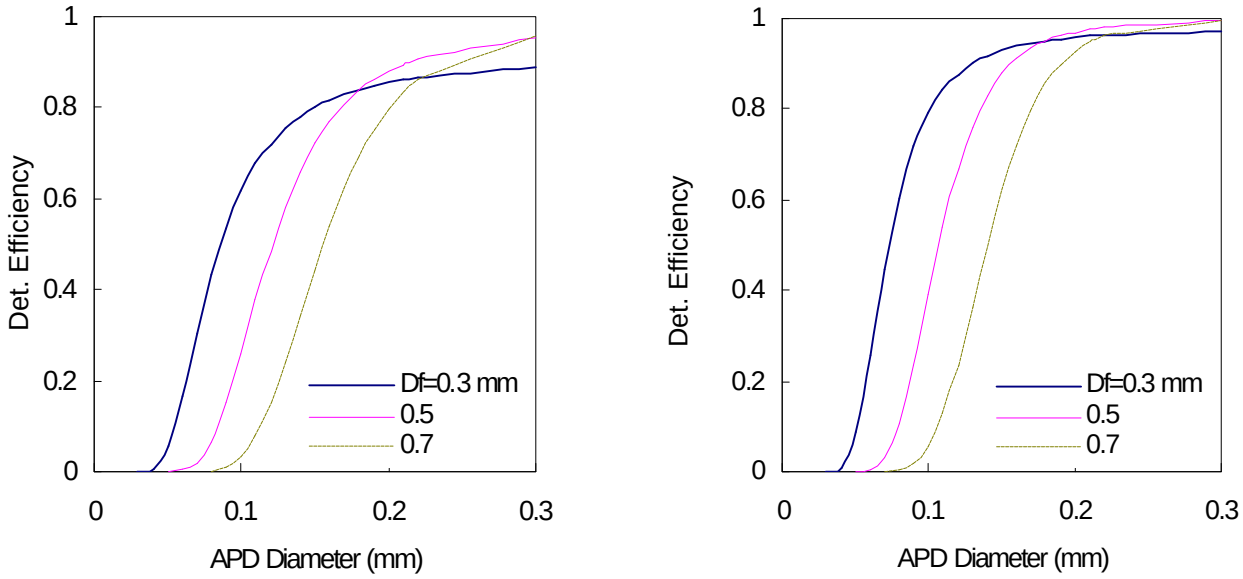

(a) (b)

Figure 10(a). Predicted lower limit of the *concentrator- mAPD* detection efficiency *versus* the μAPD active area diameter for 0.3, 0.5, and 0.7 mm diameter single-clad scintillating fibers, (3.4% scintillation trapping efficiency was assumed for single-clad fibers); (b) Predicted upper limit of the *concentrator- mAPD* detection efficiency for 0.3, 0.5, and 0.7 mm diameter multiclad scintillating fibers, (5.6% scintillation trapping efficiency was assumed for multiclad fibers). The μAPDs were biased at 3 V above the breakdown voltage.

The results show that, in order to reach high detection efficiency for multiclad fibers, the minimum μAPD size should be approximately 0.17 mm. This will require cooling the μAPD to 210K for 100 Hz dark count rate. However, the dark count rate limitation is not purely conceptual. Further μAPD fabrication improvement will decrease the leakage currents, and consequently reduce the dark count rate. The cone concentrators have the light transfer efficiency lower than expected and require further improvement of the mirror fabrication process. Improvements of the cone concentrator efficiency will shift the curves in Figure 10b toward left, thus allowing μAPD layout designs with smaller size of the active area and lower dark count rates.

5. CONCLUSIONS

The evaluation of the μAPD and concentrator performance provided us with the information required to select the detector prototype design and to predict the composite detector performance. The results show that custom layout μAPD arrays and concentrator arrays will satisfy most of the FiberGLAST requirements. The dark count rate requirement is met for somewhat lower operation temperature than desired. The conclusions, relative to the FiberGLAST requirements, are:

- Cone concentrators with simple, and potentially low cost fabrication technology, will decrease the μAPD area (and consequently the dark count rate), without inducing significant degradation of the detection efficiency;
- There is an μAPD minimum size threshold required to operate the integrated *concentrator- mAPD* detector at high detection efficiency;
- Fibers diameters ranging from 0.3 to 0.7 mm can be efficiently read out by the integrated μ*APD – concentrator* detectors with detection efficiency close to 100% for multiclad fibers;
- Simple and low cost active load passive quenching schemes allow decreasing the reset time to 1 μs at only 0.7 μW quiescent power for 100 Hz dark count rate;
- Further selection of the bipolar transistor (higher current gain) would allow biasing the μAPD at the optimal voltage above breakdown (3.5-4 V) and decrease the reset time to 0.5 μs; and
- The crosstalk for more than 450 μm pixel to pixel distance is negligible and no anti-crosstalk designs need to be implemented.

The above results show that the μAPD technology meets most of the FiberGLAST technical requirements and would have an advantage over the existing technologies in terms of performance, cost and reduced complexity. Improvements of the μAPD and cone fabrication would decrease the size of the μAPD pixels and allow operation at higher temperature.

6. AKNOWLEDGEMENTS

This research was sponsored by the contract # NASA H-29453D.

7. REFERENCES

1. G.J. Fishman, D.H. Dieter, Gamma Ray Bursts, New Observations Illuminate the Most Powerful Explosions in the Universe, *Scientific American*, pp.34-39, July 1997.
2. S. Vasile, J.S.Gordon, R. Farrell, M. R. Squillante, and G. Entine, Fast Avalanche Photodiode Detectors for Scintillating Fibers, *SCIFI 93: Workshop on Scint. Fiber Detectors*, Notre Dame IN, Eds. A.D. Bross, et al., World Scientific, Oct. 1993.
3. S. Vasile, R. J. Wilson, S. Shera, D. Shamo, M. R. Squillante, High Gain Avalanche Photodiode Arrays for DIRC Applications, submitted for publication to *IEEE Trans. Nucl. Sci.*, Oct.1998.
4. S. Vasile, P. Gothoskar, R. Farrell, D. Sdrulla, Photon Detection with High Gain Avalanche Photodiode Arrays, *IEEE Trans. Nucl. Sci*., **45**, 3, pp.720 –723, 1997.
5. R. Winston, Selected Papers on Nonimaging Optics, *SPIE Milestone Series*, **106**, 1995.
6. R.G.W. Brown, R. Jones, J.G. Rarity, and K.D. Ridley, Characterization of Silicon Avalanche Photodiodes for Photon Correlation Measurements. 2: Active Quenching, *Appl. Opt*. **26**, 12, pp. 2383,1987.
7. Bicron Data Sheet, *Scintillating Optical Fibers*,1997.
8. L. Levi, *Applied Optics*, John Wiley & Sons, 1980.
9. A. Mathewson, J.C. Alderman, J. Ryan, R.M. Redfern, G.T. Wrigson, Photon Counting Arrays for Spatially Varying, Low Light Level Signals, *Proc. SPIE*, **2022,** pp.132-143, 1993.
10. G. J. Fishman, private communication, 1998.

R.G.W., Brown, R.Jones, , J.G. Rarity, and K.D. Ridley, *Characterization of Silicon Avalanche Photodiodes for Photon Correlation Measurements. 2: Active Quenching*, Appl. Opt. 26, 12, pp. 2383,1987.
RFarrell., et al., *Large Area Silicon Avalanche Photodiodes for Scintillation Detectors*, Nucl. Instrum. & Meth. in Phys. Res., A288 pp. 137-139, 1990.
Farrell R., K. Vanderpuye and G. Entine, et al., *High Resolution, Low Energy Avalanche Photodiode X-Ray Detectors*, IEEE Trans. Nucl. Sci., 38, No. 2, pp. 144-147, April, 991.
Levi L. *Applied Optics*, John Wiley & Sons, 1980.
Luque *A. Non-Imaging Optics in Photovoltaic Concentration, Physics in Technology*, 17, pp. 118-124,1986.
Marino R., Ochoa J.R., Sanchez A., DiCecca S., Newburry N.R.and Vasile S. *3D Imaging Laser Radar with Photonic Sensitivity*, Proc. IRIS Systems, May 1996.
Mathewson A., J.C. Alderman, J. Ryan, R.M. Redfern, G.T. Wrigson, *Photon Counting Arrays for Spatially Varying, Low Light Level Signals*, Proc. SPIE, 2022, pp. 132-143 (1993).
McIntyre R.J., *Recent Developments in Silicon Avalanche Photodiodes*, Measurement, 3, pp. 146-152,1985.
Winston R. *Selected Papers on Nonimaging Optics*, SPIE Milestone Series 106, 1995.
Winton R., *Light Collection within the Framework of Geometrical Optics*, Journal of the Optical Society of America, vol. 60, num. 2, February,1970.

---

[1] G.J. Fishman, D.H. Dieter, *Gamma Ray Bursts, New Observations Illuminate the Most Powerful Explosions in the Universe*, p.34-39, July, 1997.

2. S. Vasile, J.S.Gordon, R. Farrell, M. Squillante, and G. Entine, *Fast Avalanche Photodiode Detectors for Scintillating Fibers*, SCIFI 93: Workshop on Scint. Fiber Detectors., Notre Dame IN, Oct. 1993 Eds. A.D. Bross, et al. World Scientific.
3. S. Vasile, R.J.Wilson, S. Shera, D. Shamo, M.R. Squillante, *High Gain Avalanche Photodiode Arrays for DIRC Applications*, submitted for publication to IEEE Trans. Nucl. Sci., Oct1998.
4. S. Vasile, P. Gothoskar, R. Farrell, D. Sdrulla, *Photon Detection with High Gain Avalanche Photodiode Arrays*, IEEE Trans. Nucl. Sci.,45, 3, p.720 –723, 1997.
5. R. Winston, *Selected Papers on Nonimaging Optics*, SPIE Milestone Series 106, 1995.
6. R.G.W., Brown, R.Jones, , J.G. Rarity, and K.D. Ridley, *Characterization of Silicon Avalanche Photodiodes for Photon Correlation Measurements. 2: Active Quenching*, Appl. Opt. 26, 12, pp. 2383,1987.
7. Bicron Data Sheet, *Scintillating Optical Fibers*.1997.
8. L. Levi, *Applied Optics*, John Wiley & Sons, 1980.
9. A. Mathewson, J.C. Alderman, J. Ryan, R.M. Redfern, G.T. Wrigson, *Photon Counting Arrays for Spatially Varying, Low Light Level Signals*, Proc. SPIE, 2022, pp. 132-143,1993.
10. G. J. Fishman, private communication, 1998.